

# Photoexcited Porphyrins as a Strong Suppressor of $\beta$ -Amyloid Aggregation and Synaptic Toxicity\*\*

Byung Il Lee, Seongsoo Lee, Yoon Seok Suh, Joon Seok Lee, Ae-kyeong Kim, O-Yu Kwon, Kweon Yu,\* and Chan Beum Park\*

**Abstract:** The abnormal assembly of  $\beta$ -amyloid (A $\beta$ ) peptides into neurotoxic,  $\beta$ -sheet-rich amyloid aggregates is a major pathological hallmark of Alzheimer's disease (AD). Light-induced photosensitizing molecules can regulate A $\beta$  amyloidogenesis. Multiple photochemical analyses using circular dichroism, atomic force microscopy, dot blot, and native gel electrophoresis verified that photoactivated meso-tetra(4-sulfonatophenyl)porphyrin (TPPS with  $M=2H^+$ ,  $Zn^{2+}$ ,  $Cu^{2+}$ ,  $Mn^{2+}$ ) successfully inhibits A $\beta$  aggregation in vitro. Furthermore, A $\beta$  toxicity was relieved in the photoexcited-TPPS-treated *Drosophila* AD model. TPPS suppresses neural cell death, synaptic toxicity, and behavioral defects in the *Drosophila* AD model under blue light illumination. Behavioral phenotypes, including larval locomotion defect and short lifespan caused by A $\beta$  overexpression, were also rescued by blue light-excited TPPS.

**M**edical application of photoactive chemicals is a promising therapeutic strategy for treating various diseases owing to its temporal and spatial controllability and reduced side effects.<sup>[1]</sup> Recently, optogenetic tools provide a new avenue to elucidate

brain function and neurodegenerative diseases by transferring light energy directly to the brain.<sup>[2]</sup> While the light-induced treatment using organic photosensitizers is an attractive option for curing various local diseases, only few studies tested the possibility of light-induced inhibition of Alzheimer's A $\beta$  aggregation and reduced cytotoxicity against PC12 cells.<sup>[3]</sup> Alzheimer's disease (AD) is a progressive and neurodegenerative disorder that causes neuronal cell death and a loss of cognitive ability.<sup>[4]</sup> Among pathological markers in the AD brain, extracellular amyloid plaques and intracellular neurofibrillary tangles are classical neuropathological hallmarks. The plaques are primarily composed of  $\beta$ -amyloid peptides (A $\beta$ ) derived from the sequential proteolysis of the amyloid precursor protein (APP).<sup>[5]</sup> The aggregation of soluble A $\beta$  monomers leads to the accumulation of spherical deposits known as senile plaque. Here, we explored a photo-induced suppression of A $\beta$  neurotoxicity in vivo as well as A $\beta$  aggregation in vitro by porphyrin molecules.

For several decades, numerous in vitro studies<sup>[6]</sup> on the inhibition of A $\beta$  aggregation focused on screening small organic molecules as potential candidates for the pharmacological treatment of AD.<sup>[7]</sup> To validate light-induced inhibition of A $\beta$  aggregation by meso-tetra(4-sulfonatophenyl) porphyrin (TPPS) and to unveil the interaction between the photoexcited porphyrin molecule and A $\beta$  peptide, we performed multiple photochemical analyses in vitro (Figure 1 a,b). After incubation of A $\beta$  monomer solution for 24 h, circular dichroism (CD) analysis showed a negative peak at 215 nm and a positive peak at 195 nm, which correspond to the typical peaks of  $\beta$ -sheet-rich secondary structure.<sup>[8]</sup> In the absence of TPPS, the  $\beta$ -sheet content of the A $\beta$  solution incubated under light illumination did not show any notable decrease, implying that light does not individually affect the aggregation pathway of A $\beta$ . Likewise, in the dark, the porphyrin molecule exhibited insignificant efficacy on the CD spectrum. In contrast, the CD peaks disappeared upon light illumination in the presence of TPPS, implying that the conversion of A $\beta$  monomers into  $\beta$ -sheet-packed aggregates was strongly inhibited by photoexcited TPPS.

We further investigated morphologic changes of A $\beta$  aggregates using ex situ atomic force microscope (AFM). The fully grown A $\beta$  fibrils of a few micrometer lengths were observed in A $\beta$  solution incubated without TPPS both in the dark (Figure 1 e) or under light (Figure 1 f), whereas only small-sized aggregates and a limited number of very short fibers were found in the TPPS-containing A $\beta$  solution under light illumination (Figure 1 h), but not in the dark (Figure 1 g). These results suggest strong inhibitory effects of photoexcited TPPS on the assembly of A $\beta$  peptides into fibrillar aggregates.

[\*] B. I. Lee,<sup>[†]</sup> J. S. Lee, Prof. Dr. C. B. Park  
Department of Materials Science and Engineering  
Korea Advanced Institute of Science and Technology  
335 Science Road, Daejeon 305-701 (Republic of Korea)  
E-mail: parkcb@kaist.ac.kr

Dr. S. Lee,<sup>[†]</sup> Y. S. Suh, A. Kim, Dr. K. Yu  
Neurophysiology Research Group, Bionano Center  
Korea Research Institute of Bioscience and Biotechnology (KRIBB)  
Department of Functional Genomics  
Korea University of Science and Technology (UST)  
Daejeon 305-333 (Korea)  
E-mail: kweonyu@kribb.re.kr

Dr. S. Lee<sup>[†]</sup>  
Gwangju Center, Korea Basic Science Institute (KBSI)  
Gwangju 500-757 (Korea)

Dr. O. Kwon  
Department of Anatomy, College of Medicine  
Chungnam National University, Daejeon 301-747 (Korea)

[†] These authors contributed equally to this work.

[\*\*] This work was supported by the Brain Pool program from KOFST (to S.L.), the KRIBB research initiative program, and the grants from the National Research Foundation (NRF) via the National Leading Research Laboratory (NRF-2013R1A2A1A05005468), 2014M3A9D8034462, and the Intelligent Synthetic Biology Center of Global Frontier R&D Project (2011-0031957) and from Cooperative Program for Agriculture Science and Technology Development (PJ01086401), Republic of Korea.

Supporting information for this article is available on the WWW under <http://dx.doi.org/10.1002/anie.201504310>.

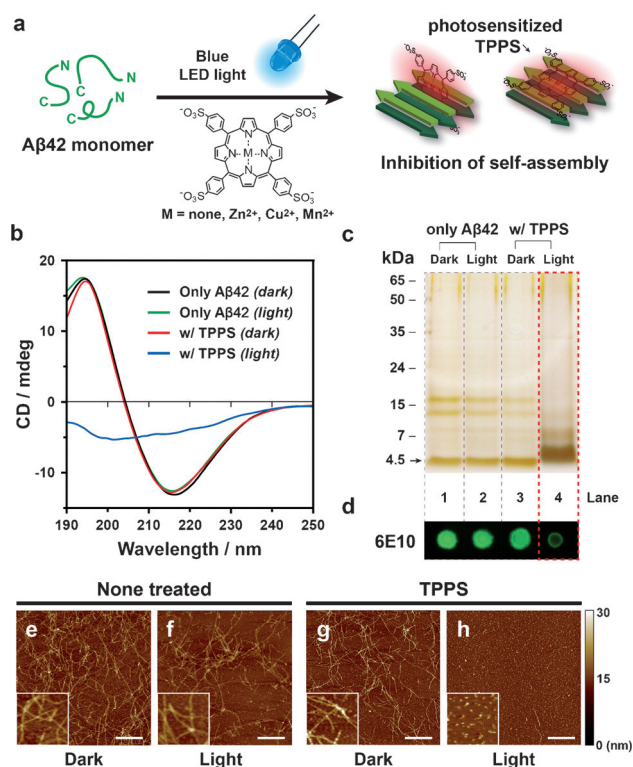


**Figure 1.** a) Diagram for inhibition of A $\beta$  self-assembly into fibril by blue LED light-sensitized TPPS. b) Analysis of photoexcited suppression on A $\beta$ 42 aggregation by CD spectroscopy. The CD spectrum clearly shows that the representative peaks of  $\beta$ -sheet structure of a peptide (195 nm and 215 nm) (black, green, and red lines) are completely disappeared by the light-induced inhibition (blue line). c) Silver-stained native gel for detecting A $\beta$ 42 monomer of 4.5 kDa. Increasing band intensity indicates that higher concentration of photo-sensitized TPPS results in higher monomeric contents of peptide in A $\beta$  solutions. d) Dot-blot assay using 6E10, A $\beta$  sequence (1–16) specific antibody. e)–h) Ex situ AFM images of A $\beta$  aggregates formed in the dark (e) and under blue LED light (f) and A $\beta$  incubated in the presence of TPPS in the dark (g) and under blue LED light (h) (see insets enlarged from panels). Scale bars: 2  $\mu$ m. The fibrillation of A $\beta$  was significantly inhibited with TPPS under the irradiation of blue LED.

We conducted native gel electrophoresis analysis to verify the blocking of A $\beta$  aggregation by photoexcited TPPS. The low intensity of the 4.5 kDa band corresponding to the A $\beta$  monomer having 42 amino acids was observed both in untreated A $\beta$  (Figure 1c, lanes 1 and 2) and TPPS-treated A $\beta$  in the dark (Figure 1c, lane 3), which is attributed to the aggregation of monomeric A $\beta$ s into fibrils of much larger molecular weight. Note that the bands for fully-grown fibers were not observed in the gel test because of their large molecular weight beyond the detection range of the native gel. In the case of the A $\beta$  incubated with TPPS under light (Figure 1c, lane 4), intense signal was monitored in the 4.5 kDa band, indicating that photoexcited TPPS significantly suppressed the aggregation of A $\beta$  monomers. A dot-blot assay result of A $\beta$  aggregates with 6E10, a human A $\beta$  (1–16)-specific antibody, is shown in Figure 1d. Only in the presence of both TPPS and light did the 24-hour-incubated A $\beta$  solution show weak reactivity against 6E10, which suggests that 6E10 epitope was possibly damaged by generated reactive oxygen

species (ROS) from TPPS photosensitization to limit antibody accessibility. The higher concentration of TPPS induced the higher degree of inhibition under light irradiation (Supporting Information, Figure S1a,b). In the CD spectra, the two peaks at 215 nm and 195 nm gradually decreased with the increasing concentration of TPPS under light and completely disappeared with 10  $\mu$ M TPPS. Consistently, the native gel electrophoresis result also showed that lesser A $\beta$  monomers aggregated with higher concentrations of TPPS (Supporting Information, Figure S2).

We verified that the variation in light wavelength also affects the inhibitory effect of TPPS. LEDs that emit three different wavelengths of light, including red ( $\lambda_{\text{max}} = 630$  nm), green ( $\lambda_{\text{max}} = 520$  nm), and blue ( $\lambda_{\text{max}} = 450$  nm), were illuminated during the incubation of A $\beta$  solutions (Figure 2a;

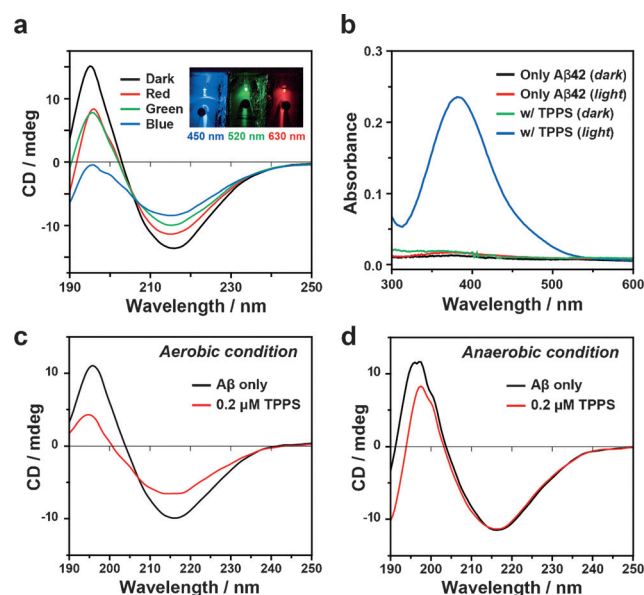


**Figure 2.** a) CD spectrum showing effect of incident light wavelength on inhibition of A $\beta$  aggregation by TPPS. (Inset: illumination of blue 450 nm, green 520 nm, and red 630 nm LED light). b) DNPH assay to detect carbonyl content in A $\beta$  samples. A peak at 380 nm indicates that the A $\beta$  sample incubated with photoexcited TPPS contains notable amounts of carbonyl contents, implying that the peptide was highly oxidized by the photosensitization. c,d) CD spectrum of A $\beta$ 42 aggregation formed under aerobic (c) and anaerobic (d) conditions in the presence of 0.2  $\mu$ M TPPS with blue-light illumination. The anaerobic experiment was conducted with an Ar-purged buffer containing 2 mM of Na $_2$ S as a singlet oxygen quencher.

Supporting Information, Figure S3). We observed a maximum hindrance effect under the blue LED, which is attributed to the optical property of TPPS (absorption maximum of TPPS = 414 nm); TPPS showed the highest degree of inhibition under the blue LED light that overlapped with its absorption band. When the power density of the light source was varied, the hindrance effect of TPPS was dependent on the intensity of incident light (Supporting Information, Figure S4).

We attribute the photoinduced anti-amyloidogenic activity of TPPS to its binding affinity to A $\beta$  and the localized

oxidative stress generated by photosensitization. According to previous work,<sup>[9]</sup> aromatic rings of small molecule inhibitors, such as polyphenols, bind competitively to the aromatic residues in A $\beta$ , preventing  $\pi$ - $\pi$  stacking of the peptide monomers, the major mechanism of amyloid fibrillation.<sup>[10]</sup> Furthermore, an electrostatic interaction between deprotonated sulfonic acid groups in TPPS ( $pK_a = 4.8$ )<sup>[11]</sup> and positively charged residues in the peptide, such as His, Lys, Arg, or NH<sub>2</sub> terminus, may also contribute to the binding affinity.<sup>[12]</sup> To investigate a possible photooxidation of A $\beta$  by TPPS, we performed a 2,4-dinitrophenylhydrazine (DNPH) assay for the detection of A $\beta$  oxidation by ROS. DNPH reacts with carbonyl groups that are generated on side chains of proteins when they are oxidized, producing 2,4-dinitrophenylhydrazone. When A $\beta$ 42 were incubated with photoexcited TPPS, they showed a new absorption peak at around 380 nm, which corresponds to the product from the DNPH reaction (Figure 2b). This result indicates that A $\beta$  peptide was strongly oxidized by TPPS under blue light. Furthermore, we observed that the inhibitory effect of photoexcited TPPS in an anaerobic environment decreased significantly (Figure 2d) compared to that in an aerobic environment (Figure 2c), which supports that ROS generation contributes to the hindrance effect of photoexcited TPPS on A $\beta$  aggregation.

Although there are a couple of reports on the in vitro study of light-driven suppression of A $\beta$  aggregation,<sup>[3]</sup> none of them investigated possible recovery of A $\beta$ -induced neural damages using in vivo model. According to our further study, TPPS rescues postsynaptic toxicity and behavior defects in the *Drosophila* AD model under blue-light illumination (Figure 3a). The *Drosophila* AD model induced by the overexpression of A $\beta$  typically exhibits multiple neurodegenerative phenotypes, such as locomotion defects, lifespan reduction, vacuolization of the brain,<sup>[13]</sup> and neuromuscular junction (NMJ) morphology defects.<sup>[14]</sup> These phenotypes can be analyzed and quantified in the *Drosophila* AD model to understand molecular mechanisms of AD pathology. Furthermore, the *Drosophila* AD model can be used to explore novel therapeutic targets of AD.<sup>[15]</sup> We found that photoexcited TPPS can reduce A $\beta$ 42 toxicity and diminish vacuole phenotype in the fly brain. In the 30 day-old fly brain, A $\beta$ 42 overexpression in the neurons (*elav* > A $\beta$ 42) showed the severe vacuole phenotype in the cell body of the brain (Supporting Information, Figure S5). In contrast, when TPPS was fed to *elav* > A $\beta$ 42 flies and excited by a blue LED light, the size and number of vacuoles were dramatically reduced compared with those of the non-TPPS-treated *elav* > A $\beta$ 42 fly brain (Supporting Information, Figure S5 f,h arrows). TPPS-treated *elav* > A $\beta$ 42 fly brains reduced the lost area by 20% (Figure 3b). According to the previous study,<sup>[16]</sup> postsynaptic overexpression of A $\beta$ 42 (*Mhc* > A $\beta$ 42) induces synaptic toxicity as shown by the loss of circa 40% NMJ synaptic boutons on muscle 6/7 of the A3 segment (Supporting Information, Figure S6a,b). This defect was rescued by the photoexcited TPPS in a concentration-dependent manner when TPPS was fed to *Mhc* > A $\beta$ 42 larvae (Figure 3c; Supporting Information, Figures S6c, S7). Since synaptic dysfunctions in *Drosophila* larval NMJ are closely related with larval locomotion behavior,<sup>[17]</sup> postsynaptic A $\beta$ 42 over-

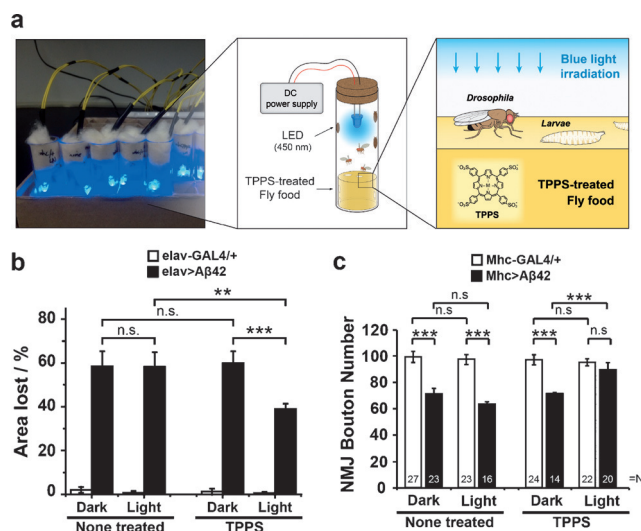


**Figure 3.** a) Blue LED light field exposure apparatus. Blue LED light-sensitized TPPS mixed with *Drosophila* food (right panel). b) Quantification of the vacuole size in adult head sections of indicated genotypes with or without TPPS treatment under dark and blue LED light. Percentage of the area lost in the cell body areas are shown as the averages  $\pm$  s.e.m. ( $n = 7$ –9 hemispheres). c) Quantification of the effect of TPPS on the total number of boutons on muscle 6/7 of A3, after normalization with bouton area. Flies of indicated genotypes were incubated with 100 nM TPPS under dark and light conditions. N indicates the number of animals analyzed. The error bars represent means  $\pm$  s.e.m. Experiments were performed at least three times. \*  $P < 0.05$ , \*\*  $P < 0.01$ , \*\*\*  $P < 0.001$ . n.s. not significant.

expression (*Mhc* > A $\beta$ 42) larvae showed a circa 30% reduction of locomotion compared to the *Mhc*-GAL4/+ control at the third instar larval stage (Supporting Information, Figure S8a,b). Importantly, photoexcited-TPPS treatment to *Mhc* > A $\beta$ 42 larvae restored the locomotion defect to the level of the control. To further explore the effects of TPPS in the *Drosophila* AD model, we examined the lifespan of flies under various conditions. Reduced maximum lifespan caused by the overexpression of A $\beta$ 42 in neurons (*elav* > A $\beta$ 42) was significantly attenuated (ca. 20%) by the photoexcited TPPS (Supporting Information, Figure S9). Consistently, photoexcited TPPS suppressed cell lethality induced by A $\beta$ 42 aggregates in a dose-dependent manner in PC12 cells according to MTT assay (Supporting Information, Figure S10). These results indicate that photoexcited TPPS can suppress A $\beta$ 42 toxicity and defects in the *Drosophila* AD model and mammalian cells. We further examined whether, after the treatment of TPPS under blue light, the reduced accumulation of A $\beta$  aggregates in vitro would be associated with decreased synaptic toxicity in *Drosophila*. Interestingly, TPPS selectively blocked the synaptic bouton loss phenotype caused by the postsynaptic overexpression of A $\beta$ 42 only under blue LED light (Supporting Information, Figure S11).

Metal ions, such as Zn<sup>2+</sup> or Cu<sup>2+</sup>, are observed in high concentration near senile plaques in the brains of AD patients,<sup>[18]</sup> thus growing interests have developed regarding the role of metal ions in A $\beta$ 42 aggregation. To explore the effects of metalloporphyrin derivatives with Zn, Cu, and Mn centers (ZnTPPS, CuTPPS, and MnTPPS) on A $\beta$  amyloido-



genesis, we monitored the effects through CD analysis in vitro and NMJ morphology in the *Drosophila* AD model, respectively. According to our results, metalloporphyrins showed different degrees of inhibition against A $\beta$ 42 aggregation under blue light (Supporting Information, Figure S12b), while negligible effects were observed in the dark (Figure S12a). For quantitative comparison, we calculated the percentage of inhibition using the CD values at 215 nm compared to that of the A $\beta$  solution incubated under dark without any porphyrin. TPPS and ZnTPPS had higher inhibitory effects on A $\beta$ 42 aggregation (44% and 47%, respectively) than those by MnTPPS and CuTPPS (17% and 15%, respectively; Figure 4a). The bouton loss phenotype caused by the postsynaptic toxicity of A $\beta$ 42 was effectively restored by ZnTPPS under blue light, but not by CuTPPS or MnTPPS (Figure 4b). ZnTPPS appeared to be more effective than TPPS in vivo, but with only a small and non-significant shift (Supporting Information, Figure S13). We attribute the variation in the degree of inhibition to the difference in the porphyrin optical properties and degree of singlet oxygen generation, rather than the effect of metal ions themselves. The photosensitized inhibition by porphyrin molecules was

affected strongly by their maximum molar extinction coefficient ( $\epsilon_{\max}$ );<sup>[19]</sup>  $\epsilon_{\max}$  of TPPS ( $5.30 \times 10^{-5} \text{ L mol}^{-1} \text{ cm}^{-1}$ ) and ZnTPPS ( $6.83 \times 10^{-5} \text{ L mol}^{-1} \text{ cm}^{-1}$ ) are higher than those of MnTPPS ( $0.95 \times 10^{-5} \text{ L mol}^{-1} \text{ cm}^{-1}$ ) and CuTPPS ( $1.91 \times 10^{-5} \text{ L mol}^{-1} \text{ cm}^{-1}$ ; Figure 4a). Furthermore, when we analyzed the formation of  $^1\text{O}_2$  under blue LED light using a singlet-oxygen sensor green (SOSG) reagent that emits fluorescence at 525 nm in the presence of  $^1\text{O}_2$ ,<sup>[20]</sup> a progressive increase in the fluorescence intensity at 525 nm was observed under light illumination for TPPS and ZnTPPS (Supporting Information, Figure S14). In the cases of MnTPPS and CuTPPS, however, the increase in accordance with the irradiation time was insignificant, indicating that the yield of  $^1\text{O}_2$  under blue LED light was much lower than TPPS and ZnTPPS. As shown in the Supporting Information, Figure S15, the triplet-state energy levels of TPPS and ZnTPPS were  $33.2 \text{ kcal mol}^{-1}$  and  $37.1 \text{ kcal mol}^{-1}$ , respectively, which are high enough to produce  $^1\text{O}_2$  with respect to ground singlet state.<sup>[19a]</sup> While TPPS and ZnTPPS have excellent fluorescent properties, emissions of MnTPPS and CuTPPS are radiationless or luminescent due to the extensive interaction between  $\pi$  electrons of the ring and the electron of central metal ion according to previous reports.<sup>[21]</sup> To examine possible incorporation of indigenous metal ions into the porphyrin ring, we investigated the interaction between TPPS and  $\text{Zn}^{2+}$  under our experimental conditions in vitro (Supporting Information, Figure S16). Our results indicate that ZnTPPS and TPPS in the presence of  $\text{Zn}^{2+}$  are photodegraded under blue light. We acknowledge that the possibility of ZnTPPS formation from TPPS and  $\text{Zn}^{2+}$  cannot be excluded. Further studies are needed to identify the photodegraded products and to unequivocally describe the interaction between  $\text{Zn}^{2+}$  and TPPS under light illumination.

In summary, photoactivated TPPS successfully inhibits A $\beta$  aggregation in vitro according to multiple photochemical analyses using CD, AFM, dot blot, and native gel electrophoresis. The light-driven efficacy against A $\beta$  aggregation is attributed to the binding affinity of TPPS to A $\beta$  and the photooxidation of A $\beta$ . Moreover, the variation in optical properties of metals in the center of porphyrin rings induced differential effect on photoinduced inhibition of A $\beta$  aggregation and its toxicity. Furthermore, we show that *Drosophila* AD model is a sensitive and suitable in vivo model system for the light-responsive chemical screening toward the suppression of A $\beta$  toxicity. We found that A $\beta$  toxicity was relieved in the photoexcited-TPPS-treated *Drosophila* AD model, which suggests high potential of TPPS as a phototherapeutic agent for treating AD. Our results provide new insights into photodynamic therapy of neurodegenerative diseases by showing that photoexcited porphyrin is an effective inhibitor against A $\beta$  toxicity. For clinical applications, further studies are needed by adapting human brain-optimized light-irradiation system.

**Keywords:** Alzheimer's disease · *Drosophila* model · photosensitizers · porphyrins ·  $\beta$ -amyloids

**How to cite:** *Angew. Chem. Int. Ed.* **2015**, *54*, 11472–11476  
*Angew. Chem.* **2015**, *127*, 11634–11638

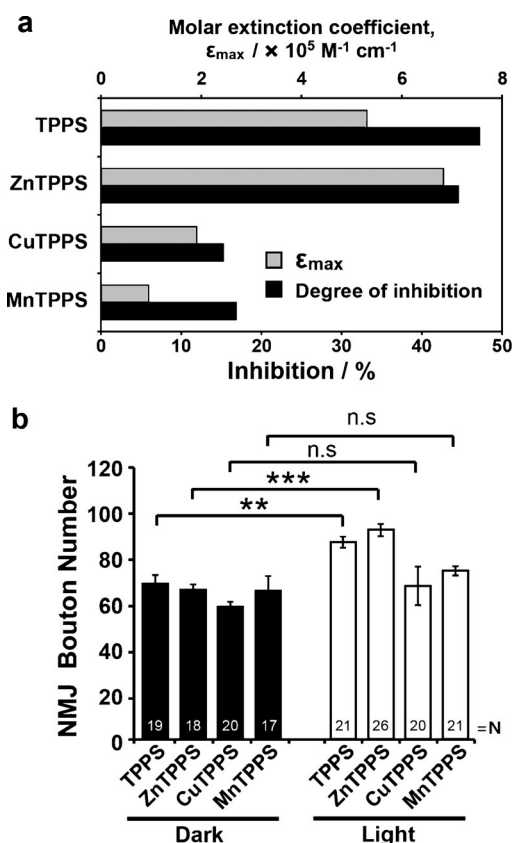


**Figure 4.** a) Degree of light-induced inhibition by different metalloporphyrins ( $10 \mu\text{M}$ ) and molar extinction coefficient at their absorbance maximum ( $\epsilon_{\max}$ ) of each porphyrins at their absorbance maxima. The inhibition degrees were calculated based on the absolute value of CD spectrum at 215 nm relative to that of the fully-grown A $\beta$  fiber. b) Quantification of NMJ bouton numbers of *Mhc* > A $\beta$ 42 by the treatment of 100 nM of TPPS, ZnTPPS, CuTPPS, and MnTPPS under dark and blue LED light. Experiments were performed at least three times. \*  $P < 0.05$ , \*\*  $P < 0.01$ , \*\*\*  $P < 0.001$ . n.s. not significant.

- [1] J. P. Celli, B. Q. Spring, I. Rizvi, C. L. Evans, K. S. Samkoe, S. Verma, B. W. Pogue, T. Hasan, *Chem. Rev.* **2010**, *110*, 2795–2838.
- [2] a) L. Fenno, O. Yizhar, K. Deisseroth, *Annu. Rev. Neurosci.* **2011**, *34*, 389–412; b) K. M. Tye, K. Deisseroth, *Nat. Rev. Neurosci.* **2012**, *13*, 251–266.
- [3] a) J. S. Lee, B. I. Lee, C. B. Park, *Biomaterials* **2015**, *38*, 43–49; b) A. Taniguchi, D. Sasaki, A. Shiohara, T. Iwatsubo, T. Tomita, Y. Sohma, M. Kanai, *Angew. Chem. Int. Ed.* **2014**, *53*, 1382–1385; *Angew. Chem.* **2014**, *126*, 1406–1409.
- [4] M. P. Mattson, *Nature* **2004**, *430*, 631–639.
- [5] D. J. Selkoe, *Trends Cell Biol.* **1998**, *8*, 447–453.
- [6] a) B. Bulic, M. Pickhardt, B. Schmidt, E. M. Mandelkow, H. Waldmann, E. Mandelkow, *Angew. Chem. Int. Ed.* **2009**, *48*, 1740–1752; *Angew. Chem.* **2009**, *121*, 1772–1785; b) E. Akoury, M. Pickhardt, M. Gajda, J. Biernat, E. Mandelkow, M. Zweckstetter, *Angew. Chem. Int. Ed.* **2013**, *52*, 3511–3515; *Angew. Chem.* **2013**, *125*, 3596–3600.
- [7] R. Mishra, B. Bulic, D. Sellin, S. Jha, H. Waldmann, R. Winter, *Angew. Chem. Int. Ed.* **2008**, *47*, 4679–4682; *Angew. Chem.* **2008**, *120*, 4757–4760.
- [8] C. J. Barrow, M. G. Zagorski, *Science* **1991**, *253*, 179–182.
- [9] R. Cukalevski, B. Boland, B. Frohm, E. Thulin, D. Walsh, S. Linse, *ACS Chem. Neurosci.* **2012**, *3*, 1008–1016.
- [10] B. Cheng, H. Gong, H. Xiao, R. B. Petersen, L. Zheng, K. Huang, *Biochim. Biophys. Acta Gen. Subj. Biochim. Biophys. Acta* **2013**, *1830*, 4860–4871.
- [11] K. Kano, *Colloid Polym. Sci.* **2008**, *286*, 79–84.
- [12] B. Salih, R. Zenobi, *Anal. Chem.* **1998**, *70*, 1536–1543.
- [13] K. Iijima, H. C. Chiang, S. A. Hearn, I. Hakker, A. Gatt, C. Shenton, L. Granger, A. Leung, K. Iijima-Ando, Y. Zhong, *PloS one* **2008**, *3*, e1703.
- [14] B. Lu, H. Vogel, *Annu. Rev. Pathol. Mech. Dis.* **2009**, *4*, 315–342.
- [15] U. B. Pandey, C. D. Nichols, *Pharmacol. Rev.* **2011**, *63*, 411–436.
- [16] S. Lee, J. W. Wang, W. Yu, B. Lu, *Nat. Commun.* **2012**, *3*, 1312.
- [17] S. D. Mhatre, V. Satyasi, M. Killen, B. E. Paddock, R. D. Moir, A. J. Saunders, D. R. Marenda, *Disease Models Mechan.* **2014**, *7*, 373–385.
- [18] a) I. W. Hamley, *Chem. Rev.* **2012**, *112*, 5147–5192; b) J. Ryu, K. Girigoswami, C. Ha, S. H. Ku, C. B. Park, *Biochemistry* **2008**, *47*, 5328–5335.
- [19] a) K. Kalyanasundaram, M. Neumann-Spallart, *J. Phys. Chem.* **1982**, *86*, 5163–5169; b) S. S. Komath, R. Kenoth, L. Giribabu, B. G. Maiya, M. J. Swamy, *J. Photochem. Photobiol. B* **2000**, *55*, 49–55.
- [20] E. S. Shibu, S. Sugino, K. Ono, H. Saito, A. Nishioka, S. Yamamura, M. Sawada, Y. Nosaka, V. Biju, *Angew. Chem. Int. Ed.* **2013**, *52*, 10559–10563; *Angew. Chem.* **2013**, *125*, 10753–10757.
- [21] M. Gouterman, in *The Porphyrins*, Vol. 3 (Ed.: D. Dolphin), Academic Press, New York, **1978**, pp. 1–156.

Received: May 12, 2015

Revised: June 22, 2015

Published online: July 14, 2015